Epitaxial Nucleation of Poly(ethylene terephthalate) by Talc: Structure at the Lattice and Lamellar Scales

H. G. Haubruge, R. Daussin, A. M. Jonas,* and R. Legras

Université catholique de Louvain, Laboratoire de Physique et de Chimie des Hauts Polymères, Croix du Sud 1, B-1348 Louvain-la-Neuve, Belgium

J. C. Wittmann and B. Lotz

CNRS-ULP, Institut Charles Sadron, Rue Boussingault 6, F-67083 Strasbourg, France

Received February 10, 2003; Revised Manuscript Received April 22, 2003

ABSTRACT: Talc has been known to nucleate poly(ethylene terephthalate) (PET) for a long time, but the exact nucleation mechanism involved had remained unknown. This study presents evidence of an epitaxial relationship between the polymer and the inorganic substrate. Electron diffraction results suggest a contact between the (100) PET plane and (001) talc basal plane as well as an alignment of the [001] PET chain axis with the three quasi-hexagonal directions of talc. Transmission electron microscopy confirms these findings but highlights some matching imperfections, partly due to irregularities of the talc lattice. Besides, it suggests a tilt of the polymer chain axis with respect to the lamellar fold surface. The long period of PET lamellar stacks is also noticeably larger on the talc contact plane.

1. Introduction

The crystallization of poly(ethylene terephthalate) (PET) from the melt is routinely accelerated by increasing its nucleation density through the use of heterogeneous nucleating agents. This industrially accounts for an important shortening of injection−molding cycles, where PET is sometimes preferred to poly(butylene terephthalate) (PBT) due to its higher thermal stability and despite the higher crystallization rate of PBT.

Succeeding a large but mostly empirical knowledge of the heterogeneous nucleation of polymers,[1] most nucleating agents and polymers were shown to interact through an epitaxial mechanism.[2] Important apparent lattice mismatches between polymer and substrate are indeed often resolved when considering the two-dimensional geometry of contact planes only. Another nucleation mechanism was also demonstrated for poly(ethylene terephthalate)[3] and other polymers,[4−6] called "chemical nucleation". In this case, a reaction between the polymer and an organic salt leads to the formation of ionic chain ends. The resulting ionic clusters are thought to precipitate and form the nuclei.

In the case of PET, chemical nucleation was shown to be the mechanism of choice for the vast majority of industrially used compounds.[3,7−9] Self-nucleation by PET crystalline remnants was also invoked as well as a physicochemical mechanism operating for some non-alkali metal hydroxides capable of water release under melt processing conditions.[10] Epitaxy of PET on heterogeneous substrates was however seldom reported,[11] and only a few studies were made on the epitaxial growth of PBT[12] or poly(decamethylene terephthalate),[13] although some aliphatic polyesters[14−16] and polyamides[16,17] were more extensively studied.

In this context, this study aims at investigating the nucleation mechanism of PET by a long-known heterogeneous nucleating agent: talc. The crystals of this phyllosilicate mineral have a high aspect ratio and few possible reactive sites located on side steps. Although it is superseded by chemical nucleating agents in terms of efficiency, its low price and its role as a filler at higher loadings lead to a continuing use of this mineral to this day.

Optical microscopy and electron diffraction results described in this paper clearly demonstrate the epitaxial behavior of PET on the large basal planes of talc. The contact planes of PET and talc are also resolved. Furthermore, staining and transmission electron microscopy (TEM) allow the direct observation of nucleated PET lamellae in spin-casted thin films. Their morphology confirms the epitaxial nature of nucleation of PET by talc and is compared to the one of virgin PET, also obtained by image analysis of TEM micrographs.

2. Experimental Section

PET (grade E47, ICI) thin films were spin-casted from a 50 g/L solution of PET in hexafluoro-2-propanol (HFIP, Acros) on freshly cleaved mica sheets covered with a 20 nm thick evaporated carbon layer. Samples for optical microscopy were spin-casted on floated glass. Talc particles were deposited on some samples from a dispersion in ethanol. It was obtained by sonicating a macroscopic grade of talc provided by Luzenac Europe, as described previously.[18]

These films, previously dried under vacuum and protected by a glass cover, were melted for 5 min at 280 °C in a Mettler Toledo FP82HT hot stage under an argon flow. They were then brought to isothermal crystallization temperature through a 20 °C/min cooling ramp. The crystallization duration was 30 min except at 230 °C, where samples were left for 60 min.

Crystallized PET films supported by carbon were floated off mica by immersion in water. Talc-nucleated samples underwent a somewhat more complicated procedure in order to reveal the talc/PET contact surfaces. A poly(acrylic acid) backing ($M_w \cong 240\,000$ g/mol, 25 wt % solution in water, Aldrich) was applied to the samples and left to dry overnight. Solidified poly(acrylic acid) droplets were scraped off the mica sheet and floated on water, with talc particles facing water. After dissolution of the backing, hydrogen fluoride (HF, 50%, Acros) was added to the bath for up to 50% of the volume in order to dissolve talc platelets. This dissolution took a few

* Corresponding author.

10.1021/ma0341723 CCC: $25.00
Published on Web 05/23/2003

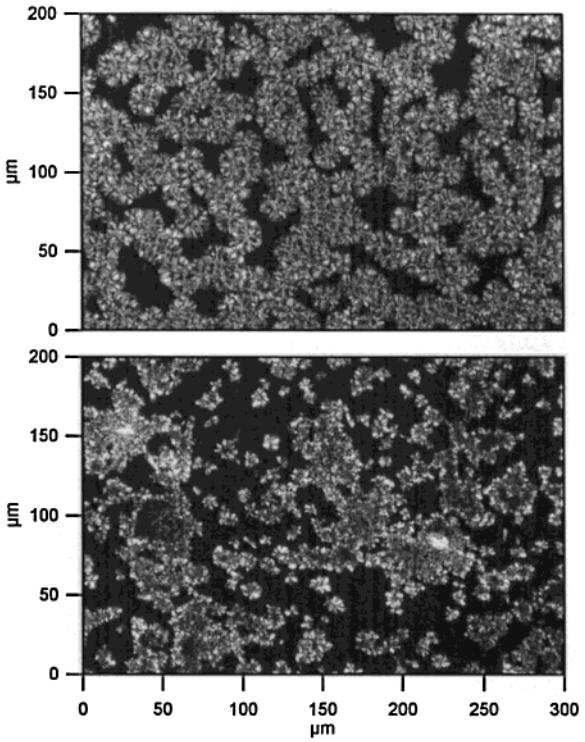

Figure 1. Polarized light optical micrographs of virgin (top) and talc-nucleated (bottom) PET thin films, crystallized at 220 °C. Large talc particles appear as darker or brighter zones in the middle of dense spherulites aggregates. Smaller particles, although present, are not readily detected at this magnification.

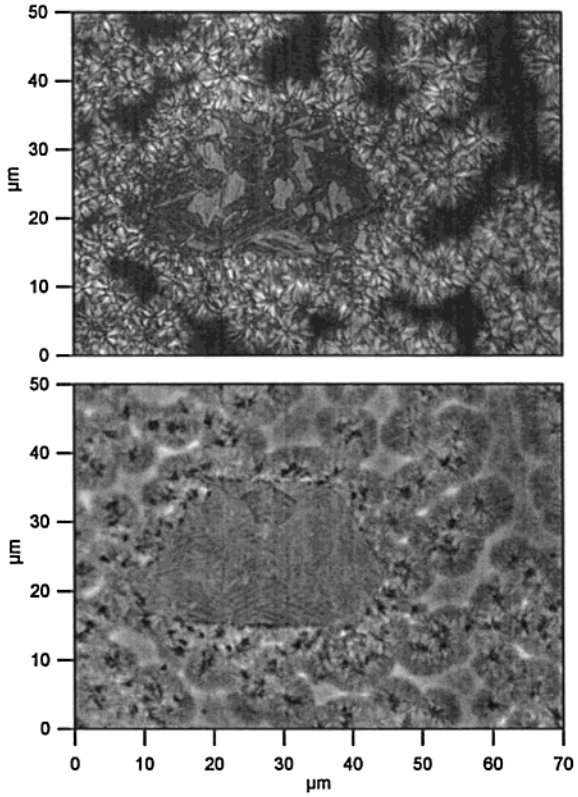

Figure 2. PET thin film, isothermally crystallized from the melt at 180 °C, nucleated by a large talc platelet. Aligned domains are noticeable on both these optical micrographs, taken under polarized light (top) and phase contrast (bottom).

hours. Floating films of both nucleated and virgin PET were retrieved on TEM copper grids.

Optical microscopy was performed on an Olympus AX70 under polarized light or using phase contrast. Electron diffraction patterns were obtained on a Philips CM12 transmission electron microscope operating at 120 kV. A simulated PET fiber pattern was obtained from the Cerius^2 software from Accelrys. Electron microscopy observations were conducted on a Philips EM 301 operating at 80 kV, after a ruthenium tetroxide staining of the samples following a previously described procedure.[19]

3. Results and Discussion

3.1. Optical Microscopy. Optical micrographs of talc-nucleated PET thin films show a very irregular spatial distribution of essentially two-dimensional spherulites compared to virgin samples crystallized in the same conditions. In both samples displayed in Figure 1, crystallization is complete. Interspherulitic gaps seen in the images result from the diffusion of molten material toward growing crystals during crystallization of the initially homogeneous film. These gaps are essentially free of polymer at the end of the crystallization process.[20] It is obvious that dense populations of spherulites cluster around the inorganic particles, while the average size of spherulites is greatly reduced by the presence of talc. This is a direct consequence of the increase in the density of nucleating sites in the vicinity of talc.

At higher magnifications, phase contrast images layer reveal the presence of locally ordered domains, on a few microns scale. These areas are also noticed in polarized light, as is shown in Figure 2. Interestingly enough, these aligned regions are oriented about 60° apart. This immediately hints to a relationship between PET chains crystallization and the quasi-hexagonal lattice structure of talc basal planes. Furthermore, the lack of any birefringence patterns observed for virgin talc particles rules out the possibility that these effects might only be due to thickness variations resulting from the cleavage of phyllosilicates planes. More decisive data are nevertheless needed in order to determine the nucleation mechanism of PET on talc.

3.2. Electron Diffraction. The electron diffraction (ED) technique allows the direct assessment of lattice relationships between polymer and nucleating substrate, far surpassing the optical shortcomings.[2] Figure 3 shows a typical selected-zone composite diffraction pattern obtained from talc-nucleated PET thin films. Alignment of the unit cell of PET with respect to the quasi-hexagonal lattice of talc is obvious.

Whereas these composite diffraction patterns can be used for the structural analysis of the talc/polymer relationship, clearer patterns can be obtained by removing the strongly diffracting substrate. Typical methods involve sublimation (in the case of low molecular weight organic compounds) or dissolution, mainly by water (in the case of alkali halides). In our case, an above-described technique adapted from Wittmann and Lotz[18] with a complementary dissolution of talc particles by hydrogen fluoride was used. This yields very clear diffraction patterns of the overgrown polymer crystals only, as shown in Figure 4.

Identification of the polymer contact plane was conducted by comparing ED patterns along different zone axes obtained by sample tilting with a PET fiber pattern simulation based on the Cerius^2 software. Unit cell parameters for this computation were taken from Daubeny et al.[21] Figure 4 displays the diffraction patterns of nucleated PET for three different tilt angles,

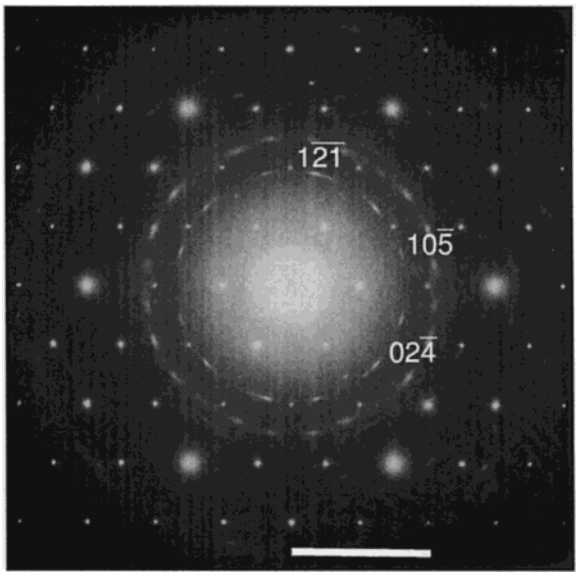

Figure 3. Composite electron diffraction pattern of nucleated PET on a talc substrate. The sharp spots originate from talc while the more diffuse arced spots are reflections from the PET crystals. Some PET reflections are indexed (caption above the corresponding spot). The scale bar corresponds to 0.5 $Å^{-1}$.

with some of the reflections indexed. Analysis of this pattern indicates that the (100) plane of PET is in contact with the (001) basal plane of talc.

Returning to the composite diffraction signal, it becomes clear that the [001] direction of the PET unit cell is parallel to the [110], [$1\bar{1}0$], and [100] directions of talc. Therefore, it is important to note that, due to the quasi-hexagonal structure of talc, these directions are 60° apart and structurally equivalent. The oriented overgrowth of PET on talc seems to be due to a lattice matching between the intermolecular chain spacing of PET (5.87 Å) and the talc hexagonal periodicity (5.28 Å). This results in a lattice mismatch of 11%, which is a little large, but still compatible with epitaxy (15%).[22] Figure 5 offers a schematic view of the alignment of PET chains with the talc basal plane.

An interesting feature of the talc/PET system is the additional symmetry forced by epitaxy unto the otherwise triclinic polymer crystals. The epitaxial relationship involves only the interchain distance of PET in the (100) plane but not the shift along the *c* axis. For any one chain orientation of PET, there exist therefore four different shifts of neighbor chains that generate two symmetrically oriented tilts of the *b* axis relative to *c* and therefore two different orientations of the unit cell that share the same *c* axis orientation. The two orientations (hereafter doublet) appear as if they were twinned, which is however not the case, since no twin plane is involved. This "doublet" is repeated three times on account of the pseudohexagonal symmetry of the talc surface, which generates therefore six orientations of the unit cell in the plane of the talc substrate. However, for each PET unit cell orientation in the plane, two orientations of the *a* axis exist (away from, or toward, the talc surface). As a result, there are 12 "unique" reflections such as [$1\bar{2}1$] in Figure 4a, for instance. In Figure 4c, it furthermore justifies the large and intense spots of the overlapping [$0\bar{1}1$] and inverted [011] reflections. Note also that the [721] zone (Figure 4b) suffers from spot bleeding from neighboring diffraction planes. This is particularly obvious for the [$0\bar{1}1$] spot, which is also weakly present in the [521] zone. Besides, the [521] zone is observed for a 0° tilt angle because of a natural inclination of the observed talc particle of about 5°.

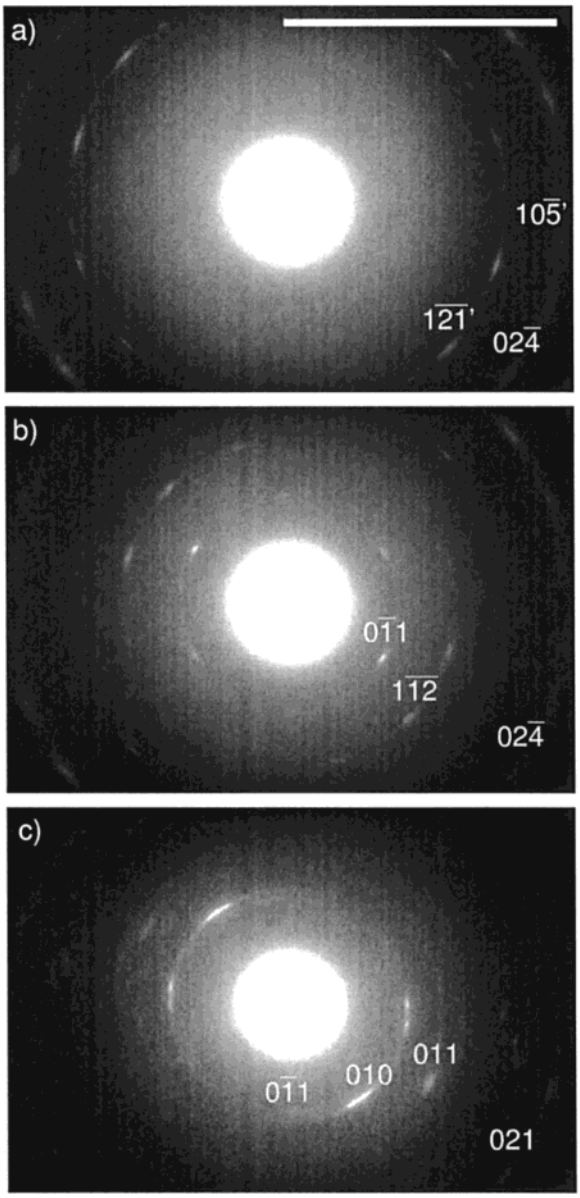

Figure 4. Electron diffraction patterns of nucleated PET obtained after dissolution of talc particles. Tilt angles are (a) 0° ([521] zone), (b) 13° ([721] zone), and (c) 40° ([100] zone). Miller indices significant of a PET (100) contact plane are indicated above the corresponding spots. The prime symbol indicates a reflection of a differently oriented unit cell. Part (a) corresponds to the low-angle region of the composite signal shown in Figure 3, thus giving the relative orientation of talc and PET lattices. The scale bar corresponds to 0.5 $Å^{-1}$.

In this section, we established the existence of an epitaxial relationship between talc basal planes and growing PET crystals. While this lattice matching was investigated in reciprocal space, further information can also be gained in direct space using adequate staining techniques to highlight PET semicrystalline morphology.

3.3. Electron Microscopy. The intrinsic anisotropy of polymer lamellar crystals, coupled with the lattice alignment between PET and talc, implies a certain amount of alignment of the polymer lamellae themselves with respect to the talc basal planes. Since the *c*-axis of PET, corresponding to its chain axis, is parallel to the three equivalent hexagonal directions of the

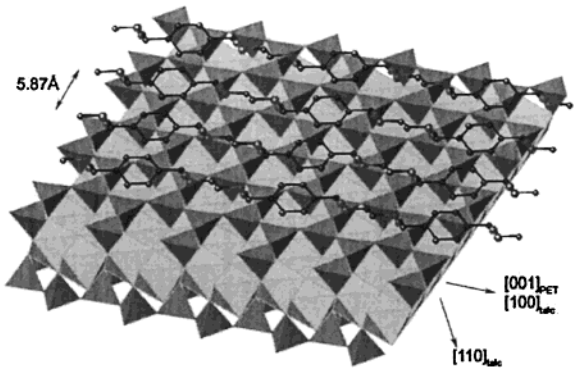

Figure 5. Schematic representation of a PET (100) plane parallel to a talc (001) basal plane. The polymer chain axis is aligned with an hexagonal direction of the substrate.

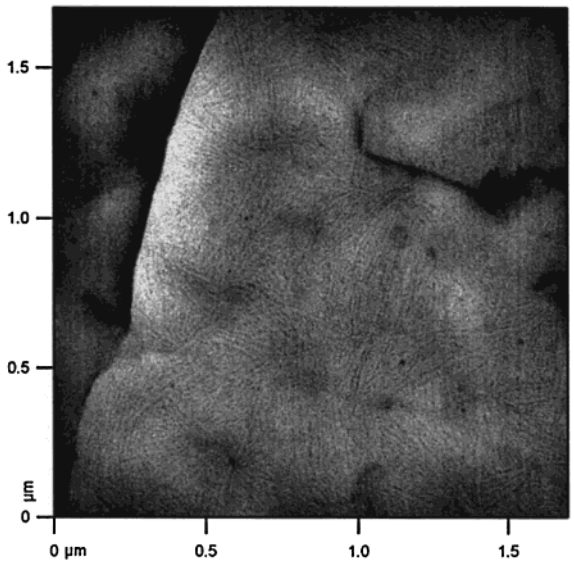

Figure 6. TEM micrograph of the talc/PET contact plane obtained from a RuO_4-stained spin-casted film where talc particles were dissolved by HF. Lamellae appear lighter than the stained amorphous regions.

mineral sheets, its lamellae are expected to lie edge-on on the inorganic substrate, with their long direction in a fixed angular relation with respect to the [110], [1$\bar{1}$0], and [100] directions of talc. This relative orientation is determined by the possible tilt of the polymer chain axis with respect to the lamellar fold plane. This tilt is indeed revealed by dissolution of talc in HF, as is shown in Figure 6. Thanks to the ruthenium tetroxide staining of the amorphous regions, lamellae growing at 60° apart are clearly visible.

While electron diffraction patterns revealed the alignment of the polymer chain axis along three talc pseudohexagonal directions, the existence of two sets of lamellae for any one of the three talc orientations is apparent on the micrographs of some samples, for instance the one depicted in Figure 6. This is made more conspicuous by considering the power spectral density of this micrograph, shown in Figure 7. This can be explained by an aforementioned tilt of the chains vs the normal to the basal plane of the lamellae. Indeed, two possible lamellar orientations correspond in this case to one chain direction, and this also allows the determination of the tilt angle itself (as projected on the (100) PET plane). Since the two sets of directions are approximately separated by a 36° angle (the complementary 24° angle seems less probable due to the dissimilar intensities of the PSD), the tilt angle can be evaluated

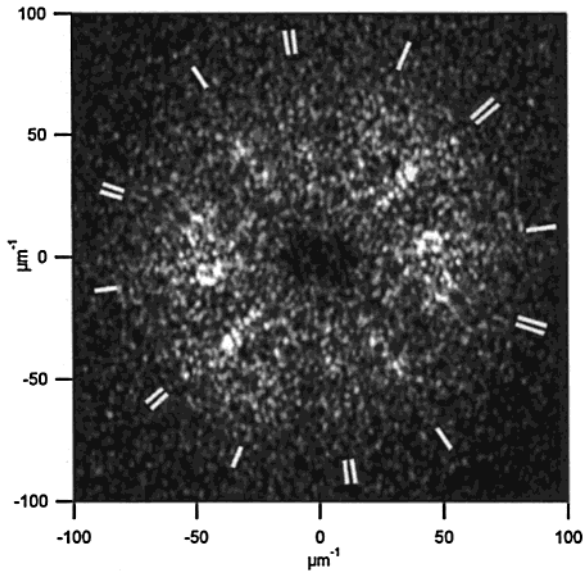

Figure 7. Power spectral density of the talc/PET contact plane micrograph shown in Figure 6. The two distinct sets of hexagonal directions are highlighted by single and double white markers, respectively.

to be about 18°. This is close to the value that can be expected if the fold plane is parallel to the (001) plane of PET.

Some relaxation of lamellar orientation is also observed. Besides long straight lamellae that are often observed on the talc contact plane, curved or shorter disturbed lamellae are also seen. Furthermore, the talc surface does not display the hexagonal symmetry. Several works have shown that deposits priviledge one or two orientations of the phyllosilicate surface (PE on talc,[18] phthalocyanines on mica[23]). This is contrary to Radoslovitch expectations and indicates a lower symmetry than hexagonal. We have also observed similar features, as can be noticed for instance in Figure 7 where lamellar directions are not equally populated, and have taken advantage of them to get further insights into the nucleation process.

The temperature dependence of the long period (L_p) of lamellae on the talc contact plane was also investigated. The results of this analysis are summarized in Figure 8. Although direct space measurements on profiles are subject to a certain amount of incertitude due to their inherent statistical poverty, clear trends emerge.

One feature is the moderate variation of the long period observed for lower crystallization temperatures. This holds true for both virgin and nucleated samples. It may be due to a crystallization taking place partly at higher temperatures, since cooling takes place at only 20 °C/min. Measured long periods thus partly correspond to lamellar stacks that already began to grow at a higher temperature.

Furthermore, L_p on talc is substantially larger than the long period on virgin thin films crystallized in the same conditions. On the contrary, L_p measured on talc-nucleated thin films but outside the talc particles is similar to the virgin samples. Besides, the difference in long periods measured for virgin and nucleated PET seems to become smaller with increasing crystallization temperature.

Tracz recently showed that lamellae of PE epitaxially grown onto graphite could reach very high thickness.[24] This behavior is similar to the present observation for

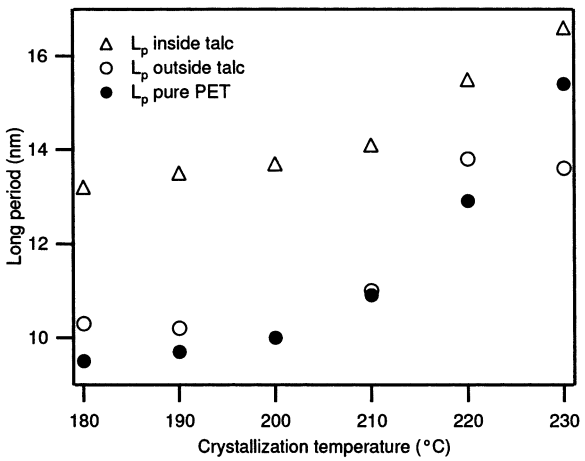

Figure 8. Crystallization temperature dependence of the long period for nucleated and virgin PET. L_p was measured inside and outside talc areas for nucleated samples. The estimated error is about 0.6 nm. The value obtained outside a talc particle for a 230 °C crystallization temperature results from measurements on one sample only and should thus be regarded as uncertain.

PET and is linked to the fact that talc provides a substrate of infinite length for crystal growth. This makes deposition and annealing along the chain much more prominent than for a conventional lamellar growth face.

4. Conclusion

Electron diffraction clearly confirms the epitaxial relationship between talc and poly(ethylene terephthalate) that could be suspected from optical microscopy results. A contact between the (100) PET plane and the (001) talc basal surface has been established as well as an alignment of the polymer chain axis with the [100], [110], and [1$\bar{1}$0] directions of talc. Although these directions are supposedly equivalent, electron micrographs of oriented lamellar stacks reveal the presence of strongly favored orientations. This reminds us of the triclinic—and not truly hexagonal—nature of the talc unit cell and of the existence of surface lattice distortions. The two sets of hexagonal directions that are sometimes noticed also indicate a tilt of the polymer chain axis with respect to the lamellar fold surface.

Apart from sodium chloride,[11] no substrate leading to the oriented overgrowth of PET had been described or published so far. (Unpublished results by Wittmann and Lotz indicate however epitaxial nucleation of PET and PBT on several organic substrates.) Although such an epitaxial behavior had been suspected by analogy with PBT or some polyamides, and the extensive study of epitaxial crystallization of PE on talc, the present results are new evidence of a seemingly ubiquitous nucleation mechanism. Furthermore, and contrary to what was once believed,[11] this new case indicates again that lattice matching does matter. Nucleation density indeed greatly increases when reasonable lattice matching is achieved.[13,25] In this context, nucleation is not initiated by surface defects, i.e., cleavage steps, on the substrate[26−28] but takes place on the whole surface of cleavage planes. It must be admitted, however, that our model experiments do not provide information on the kinetics of the nucleation process which may be affected by other parameters such as melt viscosity at the vicinity of the talc surface. To which extent such parameters may be of importance still remains to be assessed.

Let us also note that possible reactions between the polymer chains and the few reactive groups present on the phyllosilicate substrate are not completely precluded by these results. But these mechanisms would only occur concurrently with, or as precursors to, the energetically favored alignment of chains on the substrate. The driving force behind this alignment is not yet clear, but it is probably to be found in the polar or van der Waals interactions between the first adsorbed polymer segments arranged in a regular lateral packing on the substrate surface.[13]

Finally, the effect of epitaxial nucleation on the semicrystalline morphology of PET was assessed. A substantial increase of the long period is observed for lamellar stacks grown in contact with a talc basal plane. This effect disappears away from the talc surface where the bulk long period is reached, and the crystallization process has no memory of the fact that it was nucleated by talc.

Acknowledgment. Hugues Haubruge is a FNRS Research Fellow and acknolewdges the financial support of this work by the Fonds National de la Recherche Scientifique. The authors also thank Dr. G. Fourty from Luzenac Europe for kindly providing the macroscopic talc samples.

References and Notes

(1) Binsbergen, F. L. *Polymer* **1970**, *11*, 253.
(2) Wittmann, J. C.; Lotz, B. *Prog. Polym. Sci.* **1990**, *15*, 909.
(3) Legras, R.; Mercier, J. P.; Nield, E. *Nature (London)* **1983**, *304*, 432.
(4) Legras, R.; Bailly, C.; Daumerie, M.; Dekoninck, J. M.; Mercier, J. P.; Zichy, V.; Nield, E. *Polymer* **1984**, *25*, 835.
(5) Legras, R.; Leblanc, D.; Daoust, D.; Devaux, J.; Nield, E. *Polymer* **1990**, *31*, 1429.
(6) Koning, C. E.; Teuwen, L.; De Plaen, A.; Mercier, J. P. *Polymer* **1996**, *37*, 519.
(7) Garcia, D. *J. Polym. Sci., Polym. Phys. Ed.* **1984**, *22*, 2063.
(8) Gilmer, J. W.; Neu, R. P.; Liu, Y. J.; Jen, A. K.-Y. *Polym. Eng. Sci.* **1995**, *35*, 1407.
(9) Xanthos, M.; Baltzis, B. C.; Hsu, P. P. *J. Appl. Polym. Sci.* **1997**, *64*, 1423.
(10) Aharoni, S. M.; Sharma, R. K.; Szobota, J. S.; Vernick, D. A. *J. Appl. Polym. Sci.* **1984**, *29*, 853.
(11) Koutsky, J. A.; Walton, A. G.; Baer, E. *J. Polym. Sci.* **1966**, *4*, 611.
(12) Ghavamikia, H.; Rickert, S. E. *J. Mater. Sci.* **1983**, *18*, 2969.
(13) Rickert, S. E.; Baer, E. *J. Appl. Phys.* **1976**, *47*, 4304.
(14) Rickert, S. E.; Baer, E. *J. Polym. Sci., Polym. Phys. Ed.* **1978**, *16*, 895.
(15) Wittmann, J. C.; Lotz, B. *J. Polym. Sci., Polym. Phys. Ed.* **1981**, *19*, 1853.
(16) Wittmann, J. C.; Hodge, A. M.; Lotz, B. *J. Polym. Sci., Polym. Phys. Ed.* **1983**, *21*, 2495.
(17) Willems, J. *Experientia* **1967**, *23*, 409.
(18) Wittmann, J. C.; Lotz, B. *J. Mater. Sci.* **1986**, *21*, 659.
(19) Haubruge, H. G.; Jonas, A. M.; Legras, R. *Polymer* **2003**, *44*, 3229.
(20) Haubruge, H. G.; Daussin, R.; Jonas, A. M.; Legras, R. *Polymer*, in press.
(21) de Daubeny, P.; Bunn, C. W.; Brown, C. J. *Proc. R. Soc. London* **1954**, *A226*, 531.
(22) Mauritz, K. A.; Baer, E.; Hopfinger, A. J. *J. Polym. Sci., Part D: Macromol. Rev.* **1978**, *13*, 1.
(23) Uyeda, N.; Ashida, M.; Suito, E. *J. Appl. Phys.* **1965**, *36*, 1453.
(24) Tracz, A.; Jeszka, J.; Kucińska, I.; Chapel, J.-P.; Boiteux, G. *Macromol. Symp.* **2001**, *169*, 129.
(25) Wittmann, J. C.; Lotz, B. *J. Polym. Sci., Polym. Phys. Ed.* **1981**, *19*, 1837.
(26) Balik, C. M.; Tripathy, S. K.; Hopfinger, A. J. *J. Polym. Sci., Polym. Phys. Ed.* **1982**, *20*, 2003.
(27) Lovinger, A. J. *Polym. Prepr.* **1980**, *21*, 253.
(28) Rybnikar, F.; Geil, P. H. *J. Polym. Sci., Part B: Polym. Phys.* **1997**, *35*, 1807.

MA0341723